Controlling the Local Electronic Properties of Si(553)-Au through Hydrogen Doping

C. Hogan,[1,2,*] E. Speiser,[3,†] S. Chandola,[3] S. Suchkova,[3] J. Aulbach,[4] J. Schäfer,[4] S. Meyer,[4] R. Claessen,[4] and N. Esser[3]

[1]*Istituto di Struttura della Materia-CNR (ISM-CNR), via Fosso del Cavaliere 100, 00133 Rome, Italy*
[2]*Dipartimento di Fisica, Università di Roma "Tor Vergata", Via della Ricerca Scientifica 1, 00133 Roma, Italy*
[3]*Leibniz-Institut für Analytische Wissenschaften - ISAS - e.V., Schwarzschildstraße 8, 12489 Berlin, Germany*
[4]*Physikalisches Institut and Röntgen Center for Complex Material Systems (RCCM), Universität Würzburg,
Am Hubland, D-97074 Würzburg, Germany*

We propose a quantitative and reversible method for tuning the charge localization of Au-stabilized stepped Si surfaces by site-specific hydrogenation. This is demonstrated for Si(553)-Au as a model system by combining density functional theory simulations and reflectance anisotropy spectroscopy experiments. We find that controlled H passivation is a two-step process: step-edge adsorption drives excess charge into the conducting metal chain "reservoir" and renders it insulating, while surplus H recovers metallic behavior. Our approach illustrates a route towards microscopic manipulation of the local surface charge distribution and establishes a reversible switch of site-specific chemical reactivity and magnetic properties on vicinal surfaces.

Atomic wires of Au and Si that form on vicinal and nominal Si(111)-Au surfaces have been the subject of intense research in recent years [1–4]. They offer a well-defined prototype for studying interesting phenomena in (quasi-)one-dimensional systems, such as metal-insulator transitions [3], atomic magnetism [4,5], long-range spin order [6], Rashba splitting [7], and spin chain manipulation [8]. Their electronic properties can be controlled externally by changing the vicinal angle (and thereby the step morphology, terrace width, density, and composition of the metallic Au wires) [2] as well as through doping by atomic Si or Au [3,9–11] or electronic charge [8]. However, their obvious technological potential as patterned substrates for nanoelectronics [12] has not been well exploited due to the uniform metallicity of the various reconstructions.

Si(553)-Au is an archetypal vicinal case. It forms a well-ordered surface at a gold coverage of 0.48 monolayers (ML) [10,13,14] that consists of 1.48 nm wide Si(111) terraces separated by single atomic steps. Density functional theory (DFT) calculations [4,5,15] predict a geometry consisting of a double Au chain running parallel to the step edges in the middle of the terrace and a Si honeycomb chain (HC) structure at the step edge, in good agreement with x-ray diffraction experiments [14], scanning tunneling microscopy (STM) [6,16,17], and spot-profile analysis low-energy electron diffraction (SPA-LEED) [5]. The basic structure is shown schematically in Fig. 1(a). Dimerization of the Au chains gives rise to the ×2 periodicity observed with LEED and STM [6,16,17]. At low temperature (< 80 K), the surface exhibits an additional ×3 periodicity (see LEED data in Fig. 4) that is driven by charge and spin ordering within the chain of dangling bond states at the step edge

[4,6,18,19]. The combination of well-ordered metallic nanowires and ordered arrays of local magnetic moments (so-called "spin chains") on a silicon surface opens up huge possibilities for applications in surface functionalization and spintronics.

In this Letter we demonstrate, using a combination of DFT calculations and reflectance anisotropy spectroscopy (RAS) measurements, how the local electronic properties of Si(553)-Au can be reversibly controlled at room temperature by surface modification. Hydrogen adsorption is shown to (i) bring the system through a metal-insulator-metal transition in a precisely controlled way, (ii) control the electronic occupation of the Au chain, which acts as a charge reservoir, (iii) tune the optimal adsorption sites for surface
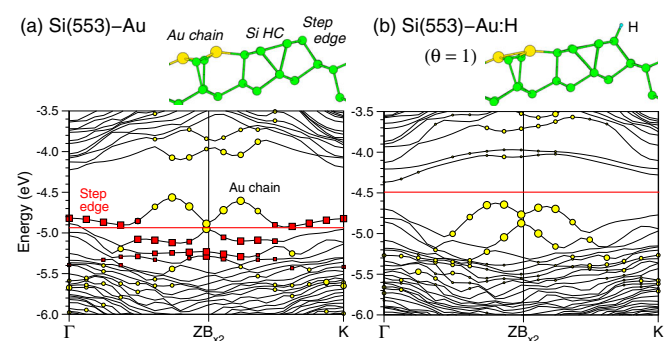
FIG. 1. Geometry (top layers only) and DFT-LDA band structure (for a ×2 cell) of (a) clean Si(553)-Au [note Si honeycomb (HC)] and (b) following step-edge passivation by hydrogen. Yellow circles indicate Au states; red squares are from Si atoms at the step edge. Energies are relative to the vacuum level. The Fermi levels are indicated by horizontal lines.

functionalization, by modifying the electronic charge distribution in the surface plane, and (iv) act as a reversible switch of the spin chain formation of the system.

We start by demonstrating, using DFT [20], the effect of H adsorption on the electronic structure of Si(553)-Au in the ×2 geometry (thus neglecting spin ordering, discussed in the Supplemental Material [22]). Atomic hydrogen is, in principle, the simplest possible adsorbate and can be regarded as a good model system for understanding chemisorption phenomena, as it is highly site specific, unlike Si [3]. The band structure of the clean surface is shown in Fig. 1(a). In agreement with previous work [15], it is a metallic system having the Fermi level cutting through bands associated with the gold chains (yellow circles) and step-edge Si atoms (red squares), respectively. Next, we passivate with atomic H both step-edge dangling bonds. As shown in Fig. 1(b), this coverage ($\theta = 1$ H atom/(×1) cell) results in an *insulating* phase, caused by a shift in the Fermi level. This is surprising: why should step-edge hydrogenation force the Au chains to lose their metallicity?

To answer this question we first examine the connection between the local geometry (Au chain and step edge) and the surface electronic charge distribution. This is achieved by systematically adding electrons to the simulation cell (system neutrality is preserved via a compensating background charge) while monitoring two representative structural parameters: the dimerization d of the Au chain, defined by $d = (a_1 - a_0)/a_0$ [see Fig. 2(a) inset], and the dihedral angle α, which quantifies the buckling of the step edge [see Fig 2(b)]. The number of electrons added during this artificial "electron doping" process is given by ρ (defined per ×1 cell). Although the precise values of d and α depend on the DFT exchange-correlation functional, the trends with respect to changes in ρ are consistent [22]. Hence, we only report results obtained using the local density approximation (LDA).

For low levels of electron doping ($\rho \leq 0.5$), the buckling angle α increases linearly with ρ before it saturates at a value very close to the corresponding angle computed for a SiH$_3^-$ molecule (52.5°). Thus α monitors the filling of the Si dangling bonds at the step edge, which dehybridize to become more s like when fully occupied (lone pair) at $\rho = 0.5$. In contrast, d remains constant up to $\rho = 0.5$, and then increases until saturation is reached at $\rho = 1.0$. Recalling the band ordering in Fig. 1(a) we conclude that d monitors filling of the Au-related bands, which occurs in the $0.5 \leq \rho \leq 1.0$ regime. Crucially, at $\rho = 1$, the system falls into an insulating state since both step-edge and Au-chain related bands are completely filled. Above $\rho = 1$, the geometry is essentially static and reflects a simple band filling of unoccupied levels as the system recovers metallicity.

This simple study [22] shows that electron doping of Si(553)-Au not only drives a metal-insulator transition, but also controls where the charge is localized within the
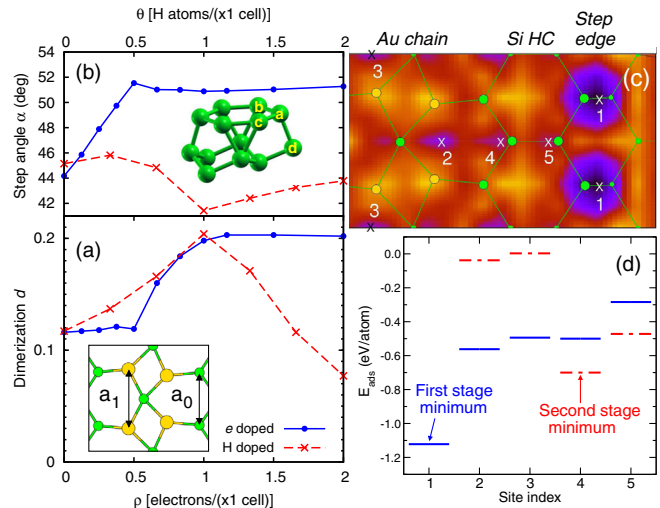
FIG. 2. (a) Au-chain dimerization d and (b) step buckling angle α, as a function of added electronic charge ρ (solid lines) and hydrogen coverage θ (dashed lines). α is the dihedral angle between planes containing atoms (a, b, c) and (b, c, d), respectively (see inset) and d is defined in the text: both are appropriately averaged within the ×2 and ×6 simulation cells. (c) Potential energy surface for H adsorption on clean Si(553)-Au, shown on the ×2 cell. Most favored sites are numbered. (d) Adsorption energy of H for the sites numbered in (c). First stage (solid lines): adsorption on the clean surface. Second stage (dashed lines): adsorption on the step-edge passivated surface (site 1 occupied).

surface. Moreover, this charge redistribution can be monitored via α and d.

We now demonstrate that almost the same charge redistribution occurs upon hydrogenation, an atomically well-defined process due to site-specific differences in adsorption energies. First, we performed DFT simulations of H adsorption across the Si(553)-Au surface in order to identify the favored sites. The potential energy surface obtained in this way is shown in Fig. 2(c), and indicates several possible adsorption sites (1–5). The adsorption energy E_{ads} [26] corresponding to each site is reported in Fig. 2(d). The step-edge dangling bond (1) is by far the most favored site (by ~0.4 eV), with Au bridging sites (2 and 3) and Si-HC sites (4 and 5) less favored. Thus, we predict a first stage of adsorption, in which H will selectively adsorb at the step edge, until the structure in Fig. 1(b) is globally obtained (passivated step edge). We then considered what would happen in a second stage of adsorption, i.e., in which the edge sites (1) are already passivated. In fact, the potential energy landscape changes dramatically, as the adsorption data in Fig. 2(d) show. In this second stage, the honeycomb sites become more active, while the Au chains remain unreactive ($E_{ads} \rightarrow 0$). Thus, step-edge hydrogenation changes the local chemical environment at the Au chains.

We then repeated our study of the surface charge distribution (as reflected by changes in α and d) but

now using the coverage θ of H (defined per $\times 1$ cell) as the control parameter [Figs. 2(a) and 2(b), dashed lines]. Although hydrogen adsorption also donates charge to the surface (thus called "H doping" henceforth), it differs significantly from electron doping as donated electrons are localized in Si-H covalent bonds, whereas e-doped charge is free to move. We show in the following, however, that the resulting electronic structure is essentially the same. Adsorption sites were filled in the order suggested by the energetics (first 1, then 4 and 5). A larger $\times 6$ cell was used to access fractional values of θ, and average values of d and α were taken. This averaging procedure, along with the local geometry perturbations (Si-H bond formation), causes α and d to show strong deviations from the electronic studies (α tends towards its value in SiH_4: $35.3°$). Nonetheless, the average dimerization smoothly increases until $\theta = 1$, whereupon the *same* value of d is obtained (indicating Au-band filling) and an insulating phase is again reached (both d and α show a cusp at this point). From an electron counting analysis [22], we deduce that Si-H bond formation causes an excess charge of $0.5e$ to be transferred from the dangling bonds to the Au chain, which is sufficient to fill the Au bands (the ability of the Au chain to act as a "charge reservoir" has previously been noted [8]). We thus conclude that, at least for the $0 \leq \theta \leq 1$ regime, H doping (i.e., H adsorption at step edge sites) controls the charge density at the Au chains. (For $\theta > 1$, H strongly perturbs the geometry at the HC sites, and thus also the Au-chain dimerization d.) These simulations predict that H doping can be used to control the surface charge distribution between step-edge states and the Au-chain reservoir.

To prove this prediction, we turn to an actual hydrogenation experiment. We use RAS, which is known to be sensitive to surface electronic states related to specific structural elements on Si-Au surfaces [27–29] and to hydrogenation on Si surfaces [30]. In experiments, the reflectance R, at near normal incidence, of light linearly polarized in two orthogonal directions is measured [31]. The RAS signal is defined by $\Delta R/R = (R_{[\bar{1}10]} - R_{[110]})/R$, where $[\bar{1}10]$ and $[110]$ correspond to directions parallel and perpendicular to the steps, respectively. Experiments were carried out in an ultrahigh vacuum (UHV) chamber, base pressure of $< 1 \times 10^{-10}$ mbar, equipped with LEED. The Si(553) sample was n type with a resistivity in the range 0.01–$0.1\ \Omega$ cm. We used direct current heating of the sample up to $1250\,°C$ to remove the protective oxide layer. Gold was deposited on the unreconstructed Si(553) surface at an elevated substrate temperature of $650\,°C$ followed by postannealing at about $850\,°C$. Long-range order of the atomic wire array was checked with LEED.

The measured RAS for the clean Si(553)-Au surface is shown in Fig. 3(a). The spectrum is characterized by a strong surface-related peak $S1$ at 2.0 eV and shoulder $S2$ at 2.7 eV. Higher energy features occurring at E_1 and E_2 are
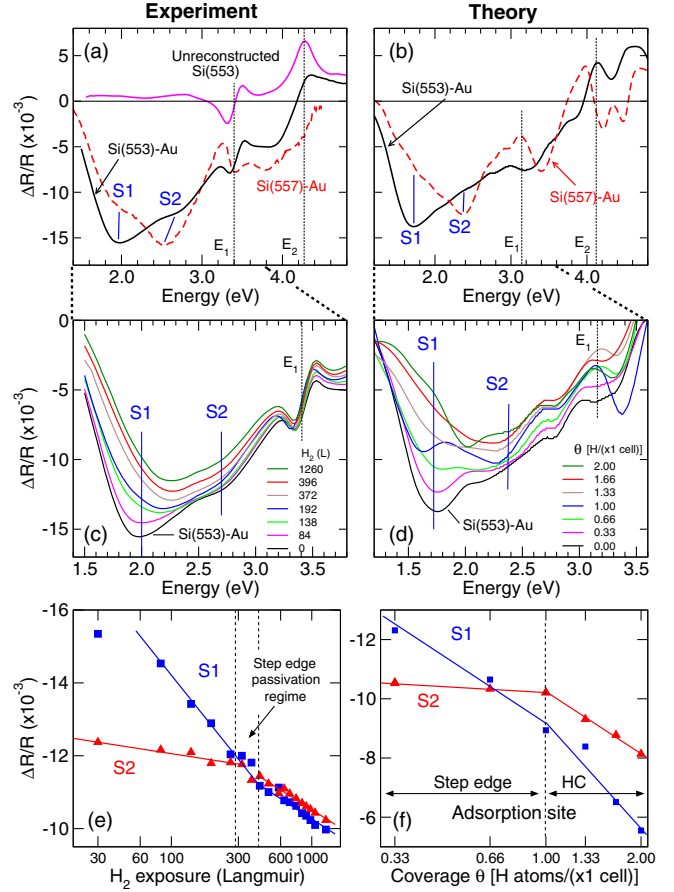
FIG. 3. Reflectance anisotropy spectra of Si(553)-Au (this work) and Si(557)-Au (Refs. [27,28]): (a) experiment (at 300K), (b) theory. RAS spectra as a function of H coverage: (c) experiment (at 300 K), (d) theory, over a smaller energy range. Transients (RAS peak intensity) of the main $S1$ and $S2$ structures as a function of H/H_2 adsorption: (e) experiment, (f) theory.

derived from bulklike transitions [also present in the unreconstructed Si(553) spectrum, as shown]. The computed spectrum [32] is shown in Fig. 3(b), and bears a good overall agreement with the experiment. The rigid redshift of about 0.3 eV is due to our use of DFT-LDA eigenvalues, and spectra are less well converged above E_1 where long-range strain effects may be present [33]. Analysis of the computed spectra indicates that $S1$ arises from transitions between occupied dangling bond states and empty Si honeycomb states, while $S2$ derives from pure honeycomb states ($\pi \leftrightarrow \pi^*$ transitions). These transitions are also present in the measured and computed spectra of Si(557)-Au [28], a single Au-chain reconstruction, reported here for comparison. Hence, RAS offers a site-specific probe of H adsorption, being sensitive to perturbations at the most favored sites at the edge (via $S1$) as well as the HC (via $S1$ and $S2$).

The Si(553)-Au surface was then exposed to hydrogen at room temperature. The UHV chamber (base pressure 1×10^{-10} mbar) was back filled with 2×10^{-7} mbar of

ultrapure (99.999%) H_2 through a leak valve. Experiments with and without a heated filament were performed, in order to compare the efficiency of molecular and atomic hydrogen. Surprisingly, no difference in RAS spectra was observed. Hence, it can be concluded that molecular hydrogen is catalytically dissociated by the Si step edge on the Si(553)-Au surface. Barrierless dissociation of molecular hydrogen has been reported to occur at other step edges of Si [34].

RAS spectra were measured at room temperature as a function of hydrogen exposure. Figure 3(c), now focused on a more surface-sensitive energy range, shows that the RAS spectra gradually attenuate with increasing coverage. The $S1$ minimum quenches more quickly than $S2$ and shifts to higher energy, which may suggest the emergence of a third spectral component around 2.3 eV. To allow a straightforward comparison with the calculated spectra, we plot the RAS amplitudes at two fixed energies (2.0 and 2.7 eV) as a function of exposure to H_2 [Fig. 3(e)]. Computed spectra and transients are shown in Figs. 3(d) and 3(f). Although our simulations are limited by considering only one adsorption configuration for each θ, they capture the essential trends in the measured data. By considering the different behaviors and site-specific sensitivities of $S1$ and $S2$, we can generally confirm our predicted two-stage process: (i) an initial stage characterized by rapid hydrogen uptake at dangling bonds at the step edge, as indicated by a fast quenching of the $S1$ RAS peak (which derives from optical transitions involving these states); (ii) a second stage, attributed to adsorption on terrace (honeycomb) sites, is accompanied by a slower quenching of both $S2$ and $S1$ RAS peaks, and hence has a slower adsorption rate. We deduce that the inflection point in the measured transient indicates full coverage of the step edge by hydrogen, giving an approximate value of exposure of the surface to hydrogenation of 330 L. Note that the procedure is completely reversible: a moderate annealing at ~900 °C causes the RAS signal of clean Si(553)-Au to be fully recovered.

These results demonstrate that H adsorption offers a quantifiable, reversible control parameter of the Si(553)-Au surface physicochemical properties. First, selective H adsorption at the step edge changes the electronic charge distribution within the surface rather than inducing major structural changes ("H doping"). In particular, it can be used to precisely tune the system between metallic and insulating phases, which can be useful for nanoelectronics. Second, an even more apparent effect upon step-edge hydrogenation is the suppression of the additional threefold periodicity that appears at low temperatures [see LEED patterns in Fig. 4(a)], attributed to spin chain formation [4]. As the process is reversible due to thermal H desorption, hydrogenation could be used as a simple switch of charge order on the step edge.

Third, the control of the local distribution of surface charge offers potential for selective molecular adsorption
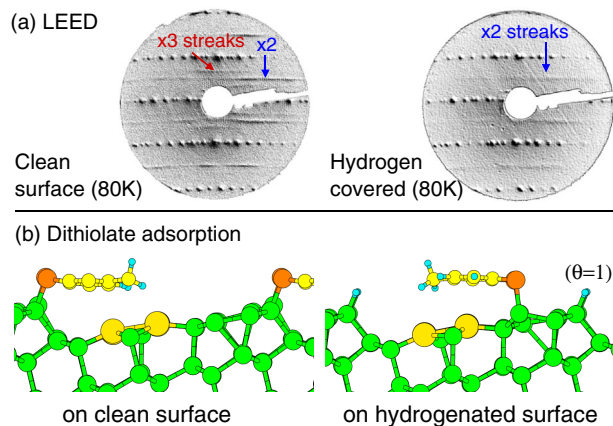
FIG. 4. Surface control through hydrogenation. (a) Step-edge charge ordering (spin chain formation), manifested as ×3 streaks in LEED measured at 80 K, is destroyed after room temperature H deposition and cooling again to 80 K. (b) Orientation of a chemisorbed organic molecule (and its dipole) is rotated by switching the favored adsorption site from the step edge to the terrace via a H coverage of $\theta = 1$.

and chemical reactivity. Use of tunable, well-characterized 1D Au-nanostructured surfaces as a template for organic self-assembled molecular growth could combine the advantages of 1D systems and organic conductors, eventually yielding molecular layers that inherit the one dimensionality of the underlying structure. Previous studies on nominal Si(111)-Au noted the tendency for molecules to adsorb on its (hardly well controlled) step edges [35] or to destabilize the Au-nanostructured phase completely [36]. By controlled saturation of specific adsorption sites, however, molecules can be induced to arrange in specific nanoscale patterns. As an example, we carried out an adsorption study [37] of an isolated dithiolate molecule on Si(553)-Au, before and after passivating the surface with hydrogen. On the clean surface, the molecule preferentially adsorbed flat over the Au chains through S—Si bonds to the step edge, as shown in Fig. 4(b). By selectively passivating the step-edge sites, the dithiolate is made to adsorb on the terrace in a rotated geometry. Direct bonding of S to Au was not observed in this case. However, molecules containing different functional groups may show further selectivity.

Finally, we note that these results apply equally to other Si(111)-Au derivatives that show a gap in the electronic band structure near the Fermi level [Si(557)-Au [28], nominal Si(111)-Au [38]], and exhibit uniformly similar RAS spectra with structurally specific optical fingerprints [28,29]. Electron counting analysis of these systems indicates that the electron deficit is uniformly $1e/(\times 1)$ cell, which makes atomic hydrogen particularly suitable for surface modification, thus opening new routes for controlling electronic states in these and related nanopatterned surfaces.

---

*conor.hogan@ism.cnr.it
†eugen.speiser@isas.de

[1] F. J. Himpsel, K. N. Altmann, R. Bennewitz, J. N. Crain, A. Kirakosian, J.-L. Lin, and J. L. McChesney, J. Phys. Condens. Matter **13**, 11097 (2001).

[2] J. N. Crain, J. L. McChesney, F. Zheng, M. C. Gallagher, P. C. Snijders, M. Bissen, C. Gundelach, S. C. Erwin, and F. J. Himpsel, Phys. Rev. B **69**, 125401 (2004).

[3] W. H. Choi, P. G. Kang, K. D. Ryang, and H. W. Yeom, Phys. Rev. Lett. **100**, 126801 (2008).

[4] S. C. Erwin and F. J. Himpsel, Nat. Commun. **1**, 58 (2010).

[5] B. Hafke, T. Frigge, T. Witte, B. Krenzer, J. Aulbach, J. Schäfer, R. Claessen, S. C. Erwin, and M. Horn-von Hoegen, Phys. Rev. B **94**, 161403 (2016).

[6] J. Aulbach, J. Schäfer, S. C. Erwin, S. Meyer, C. Loho, J. Settelein, and R. Claessen, Phys. Rev. Lett. **111**, 137203 (2013).

[7] L. V. Bondarenko, D. V. Gruznev, A. A. Yakovlev, A. Y. Tupchaya, D. Usachov, O. Vilkov, A. Fedorov, D. V. Vyalikh, S. V. Eremeev, E. V. Chulkov, A. V. Zotov, and A. A. Saranin, Sci. Rep. **3**, 1826 (2013).

[8] J. Aulbach, S. C. Erwin, R. Claessen, and J. Schäfer, Nano Lett. **16**, 2698 (2016).

[9] A. Kirakosian, J. Crain, J.-L. Lin, J. McChesney, D. Petrovykh, F. Himpsel, and R. Bennewitz, Surf. Sci. **532–535**, 928 (2003).

[10] I. Barke, F. Zheng, S. Bockenhauer, K. Sell, V. Oeynhausen, K. Meiwes-Broer, S. Erwin, and F. Himpsel, Phys. Rev. B **79**, 155301 (2009).

[11] I. Barke, S. Polei, V. v. Oeynhausen, and K-H. Meiwes-Broer, Phys. Rev. Lett. **109**, 066801 (2012).

[12] R. Bennewitz, J. N. Crain, A. Kirakosian, J.-L. Lin, J. L. McChesney, D. Y. Petrovykh, and F. J. Himpsel, Nanotechnology **13**, 499 (2002).

[13] S. Ghose, I. Robinson, P. Bennett, and F. Himpsel, Surf. Sci. **581**, 199 (2005).

[14] W. Voegeli, T. Takayama, T. Shirasawa, M. Abe, K. Kubo, T. Takahashi, K. Akimoto, and H. Sugiyama, Phys. Rev. B **82**, 075426 (2010).

[15] M. Krawiec, Phys. Rev. B **81**, 115436 (2010).

[16] J. R. Ahn, P. G. Kang, K. D. Ryang, and H. W. Yeom, Phys. Rev. Lett. **95**, 196402 (2005).

[17] P. C. Snijders, S. Rogge, and H. H. Weitering, Phys. Rev. Lett. **96**, 076801 (2006).

[18] K. Biedermann, S. Regensburger, T. Fauster, F. J. Himpsel, and S. C. Erwin, Phys. Rev. B **85**, 245413 (2012).

[19] P. C. Snijders, P. S. Johnson, N. P. Guisinger, S. C. Erwin, and F. J. Himpsel, New J. Phys. **14**, 103004 (2012).

[20] We used the QUANTUM-ESPRESSO code [21], repeated slabs of 6–10 layers separated by vacuum, and a framework of plane waves and norm-conserving pseudopotentials. Kinetic energy cutoff was 50 Ry. $(2 \times 4 \times 1)$ and $(1 \times 2 \times 1)$ **k**-point grids were used for (1×2) and (1×6) cells, respectively.

[21] P. Giannozzi *et al.*, J. Phys.: Condens. Matter **21**, 395502 (2009).

[22] See Supplemental Material at http://link.aps.org/supplemental/10.1103/PhysRevLett.120.166801 for a discussion on the roles of spin [22] and exchange-correlation functional (including PBE [23]) on the results, as well as detailed electron counting analysis [24].

[23] S. C. Erwin and P. C. Snijders, Phys. Rev. B **87**, 235316 (2013).

[24] J. P. Perdew, K. Burke, and M. Ernzerhof, Phys. Rev. Lett. **77**, 3865 (1996).

[25] S. C. Erwin and H. H. Weitering, Phys. Rev. Lett. **81**, 2296 (1998).

[26] Adsorption energies defined as $E_{ads} = E_{slab+H} - E_{slab} - 1/2E_{H_2}$.

[27] N. McAlinden and J. F. McGilp, Europhys. Lett. **92**, 67008 (2010).

[28] C. Hogan, N. McAlinden, and J. F. McGilp, Phys. Status Solidi (b) **249**, 1095 (2012).

[29] C. Hogan, E. Ferraro, N. McAlinden, and J. F. McGilp, Phys. Rev. Lett. **111**, 087401 (2013).

[30] M. Palummo, N. Witkowski, O. Pluchery, R. Del Sole, and Y. Borensztein, Phys. Rev. B **79**, 035327 (2009).

[31] D. E. Aspnes and A. A. Studna, Phys. Rev. Lett. **54**, 1956 (1985).

[32] Optical spectra are computed from the slab and bulk dielectric functions, computed at the independent particle level using the YAMBO code, A. Marini, C. Hogan, M. Grüning, and D. Varsano, Comput. Phys. Commun. **180**, 1392 (2009), with (16×8) and (4×4) *k*-point meshes for the (1×2) and (1×6) cells, respectively. Further detail is given in Refs. [27,28].

[33] L. K. Béland, E. Machado-Charry, P. Pochet, and N. Mousseau, Phys. Rev. B **90**, 155302 (2014).

[34] P. Kratzer, E. Pehlke, M. Scheffler, M. B. Raschke, and U. Höfer, Phys. Rev. Lett. **81**, 5596 (1998).

[35] F. Zheng, I. Barke, X. Liu, and F. J. Himpsel, Nanotechnology **19**, 445303 (2008).

[36] J. Kautz, V. Janssen, R. Tromp, and S. van der Molen, Surf. Sci. **632**, L18 (2015).

[37] S. Suchkova, C. Hogan, F. Bechstedt, E. Speiser, and N. Esser, Phys. Rev. B **97**, 045417 (2018).

[38] S. G. Kwon and M. H. Kang, Phys. Rev. Lett. **113**, 086101 (2014).